



LUND UNIVERSITY

Development of Feedback Microwave Thermotherapy in Symptomatic Benign Prostatic Hyperplasia.

Schelin, Sonny

2006

[Link to publication](#)

Citation for published version (APA):

Schelin, S. (2006). *Development of Feedback Microwave Thermotherapy in Symptomatic Benign Prostatic Hyperplasia*. [Doctoral Thesis (compilation), Urology]. Department of Urology, Clinical Sciences, Lund University.

Total number of authors:

1

General rights

Unless other specific re-use rights are stated the following general rights apply:

Copyright and moral rights for the publications made accessible in the public portal are retained by the authors and/or other copyright owners and it is a condition of accessing publications that users recognise and abide by the legal requirements associated with these rights.

- Users may download and print one copy of any publication from the public portal for the purpose of private study or research.
- You may not further distribute the material or use it for any profit-making activity or commercial gain
- You may freely distribute the URL identifying the publication in the public portal

Read more about Creative commons licenses: <https://creativecommons.org/licenses/>

Take down policy

If you believe that this document breaches copyright please contact us providing details, and we will remove access to the work immediately and investigate your claim.

LUND UNIVERSITY

PO Box 117
221 00 Lund
+46 46-222 00 00

EVALUATION OF MICROWAVE THERMOTHERAPY WITH HISTOPATHOLOGY, MAGNETIC RESONANCE IMAGING AND TEMPERATURE MAPPING

CHRISTIAN HUIDOBRO,* MAGNUS BOLMSJÖ,† THAYNE LARSON,‡ JEAN DE LA ROSETTE,§
LENNART WAGRELL,† SONNY SCHELIN,† TOMASZ GORECKI AND ANDERS MATTIASON||

From the Department of Urology, University of Chile (CH), Santiago, Chile, Radiation Physics Department, Lund University (MB), ProstaLund Operations AB (MB) and Department of Urology, Lund University Hospital (AM), Lund, Department of Urology, University Hospital of Uppsala (LW), Uppsala and Departments of Surgery and Pathology, County Hospital of Kalmar (SS, TG), Kalmar, Sweden, Department of Urology, Mayo Clinic Scottsdale (TL), Scottsdale, Arizona, and Department of Urology, Academic Medical Center, University of Amsterdam (JdIR), Amsterdam, The Netherlands.

ABSTRACT

Purpose: Interstitial temperature mapping was used to determine the heat field within the prostate by the Coretherm (ProstaLund, Lund, Sweden) transurethral microwave thermotherapy device. Gadolinium enhanced magnetic resonance imaging (MRI) and histopathology were used to determine the extent and pattern of coagulation necrosis following treatment. The cell kill assessment feature of the device was compared with MRI and histopathology.

Materials and Methods: A total of 12 patients were treated, including 5 with adenocarcinoma of the prostate and 7 with benign prostatic hyperplasia. Temperature sensors were inserted from the perineum to map the temperature distribution. The 5 patients with adenocarcinoma underwent prostatectomy and subsequent histopathology 3 to 6 weeks after treatment. MRI and cell kill calculations were performed in all patients.

Results: Therapeutic temperatures were found in a bowl-like shape with a wide circumference of highest temperatures at the base of the prostate, and decreasing temperature and circumference toward the apex. Tissue necrosis assessed by histopathology, MRI and cell kill calculations overlapped reasonably well in shape and size. Histopathology showed that the prostatic urethra was destroyed by treatment.

Conclusions: Coretherm microwave treatment causes significant tissue necrosis of the prostate, bladder neck and urethral mucosa. The cell kill calculation provides an on-line estimate of the amount of necrosis caused during treatment.

KEY WORDS: prostate, prostatic neoplasms, prostatic hypertrophy, necrosis, microwaves

The aging prostate accounts for many urological diseases in men, including benign prostatic hyperplasia (BPH), prostatic carcinoma and prostatitis. With office based treatment protocols that require no hospitalization transurethral microwave thermotherapy (TUMT) has become an attractive alternative to surgical treatments.¹ Recent clinical studies of the Coretherm TUMT device have shown comparable results in relief of obstruction and lower urinary tract symptoms between TUMT and transurethral prostatic resection (TURP), while the rate of adverse events requiring hospital intervention was significantly lower for TUMT than for TURP (2% vs 17%).^{2,3}

Generally microwave treatment creates high temperatures deep within the prostate to ablate the tissue and destroy α receptors.⁴ The process is governed by tissue temperature and the duration of heat exposure.⁵ For a long time the temperature-time threshold determined by Henriques⁶ has been the standard by which to assess thermal damage. A recent study by Bischof et al from Minneapolis revealed new

data on the heat sensitivity of human BPH tissue.⁷ For prostate stromal tissue the threshold for causing heat necrosis is about 60 minutes at 45C, 5 minutes at 55C, 2 minutes at 60C and 1 minute at 70C. Glandular epithelium cells appear more sensitive. Heat damage occurs after 15 minutes at 50C or 5 minutes at 55C.⁷

Tissue temperature depends on the heat field of the microwave antenna, tissue cooling by blood flow, the spread of heat due to heat conduction and urethral cooling, if any.⁵

A TUMT device, namely the Coretherm catheter, includes a needle-like temperature probe that protrudes into 1 of the lateral lobes of the prostate and contains 3 sensors that monitor intraprostatic temperatures during treatment. It gives the physician the ability to adjust the energy level and customize treatment to the individual. The device calculates the volume of necrosis by combining measured intraprostatic temperatures with tissue heat sensitivity, delivered microwave power and antenna radiation pattern.

In a retrospective study of 22 patients who underwent ProstaLund treatment Schelin reported a mean calculated cell kill of 27 ml during ongoing treatment vs a mean prostate shrinkage of 26 ml on 2-dimensional transrectal ultrasound (TRUS) at 3 months of followup.⁸ In a prospective study of 33 patients Hoffman et al compared cell kill calculations with the prostate shrinkage measured by 3-dimensional ultrasound 3, 6 and 12 months after treatment.⁹ They found that the cell kill calculations were precise to within ± 8 gm in 90% of the cases.

Accepted for publication September 5, 2003.

Study received local ethics committee approval.

* Financial interest and/or other relationship with ProstaLund, Urologix and Abbott Laboratories.

† Financial interest and/or other relationship with ProstaLund.

‡ Financial interest and/or other relationship with ProstaLund, BSC, Urologix, Injctx, ATI and Johnson and Johnson-Ethicon.

§ Financial interest and/or other relationship with ProstaLund, Bard, BSC and American Medical Systems.

|| Financial interest and/or other relationship with ProstaLund, Pharmacia, Eli Lilly and Ferring.

However, few studies have been done in which intraprostatic temperature is related to histopathology and/or magnetic resonance imaging (MRI) of the prostate.^{10–12} MRI with gadolinium contrast material can be used to visualize the heat coagulated zone. Necrotic tissue appears dark in areas of absent or decreased perfusion.¹²

In the current study we investigated if histopathology, MRI and cell kill calculations based on intraprostatic temperature are useful for assessing necrosis after TUMT.

MATERIAL AND METHODS

The current series was designed as an open study done at the Department of Urology, University of Chile, Santiago, Chile. A total of 12 patients were treated with the Coretherm TUMT device. Patients provided informed consent to participate. All patients were investigated with a history, International Prostate Symptom Score, free urinary flow, cystoscopy, urinary and blood chemistry including prostate specific antigen and TRUS of the prostate. Prostate size was 18 to 76 ml (mean 48). Patient age was 56 to 80 years (mean 67). Retropubic radical prostatectomy was performed 1 week after TUMT in 5 patients with diagnosed localized prostate cancer. The other 7 patients were diagnosed with BPH. Patients were treated according to a scheme (table 1).

In all 3 patient groups the Coretherm temperature probe was used by the physician to control the delivered microwave power setting (fig. 1). Microwave power (maximum 80 W) was varied to achieve therapeutic temperatures in the prostate (45°C or greater). Treatment was terminated when the calculated cell kill reported by the device was between 20% and 50% of prostate volume. Extensive thermal mapping was performed in groups 1 and 2. Eight 1.8 mm closed-end nylon tubes were inserted into the prostate from the perineum under x-ray and/or TRUS guidance. Six to 8 temperature probes containing 5 transducers each separated by 10 mm (ie, a total of 30 to 40 measuring points) were inserted into the nylon carrier tubes to measure intraprostatic temperatures between the base and apex at varying radial distances from the urethra (3 to 25 mm). Figures 2 and 3 show typical positions of the carrier tubes.

One to 14 days (mean 6) prior to and 4 to 16 days after TUMT all patients (groups 1 to 3) were examined with gadolinium enhanced MRI using a 1.5 Tesla Magnetom (Siemens Medical Systems, Inc., Iselin, New Jersey). The volume of the perfusion defect on MRI was used to quantify the volume of necrosis.

Patient group 1 underwent radical retropubic prostatectomy one week after TUMT. The harvested prostates were fixed in 10% buffered formalin. Serial 5 mm transverse tissue sections were prepared from the prostatic apex to the base. Sections were exposed to graded alcohols and xylene, embedded in paraffin, cut at 5 μ m, stained with hematoxylin and

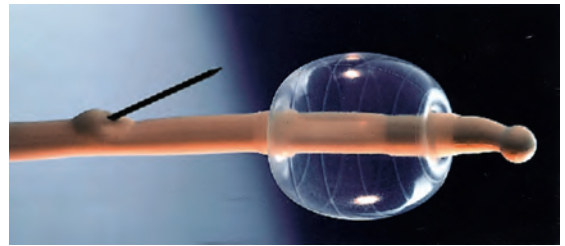


FIG. 1. ProstaLund Coretherm catheter has built-in temperature probe that protrudes into prostate from catheter. Probe contains 3 temperature transducers to map temperature distribution along probe.

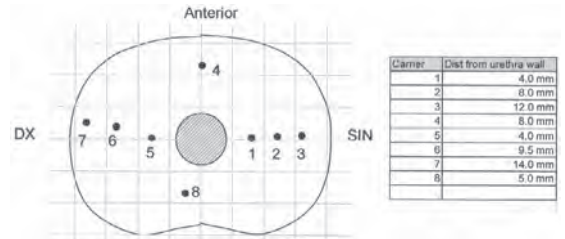


FIG. 2. Transverse prostate section with typical locations (numbered circles) of carrier tubes for temperature probes. It is general picture only since exact positions on x-ray or TRUS varied slightly among patients. Gray lines represent 5 mm indicators. *Dx*, dexter. *SIN*, sinister. *Dist*, distance.

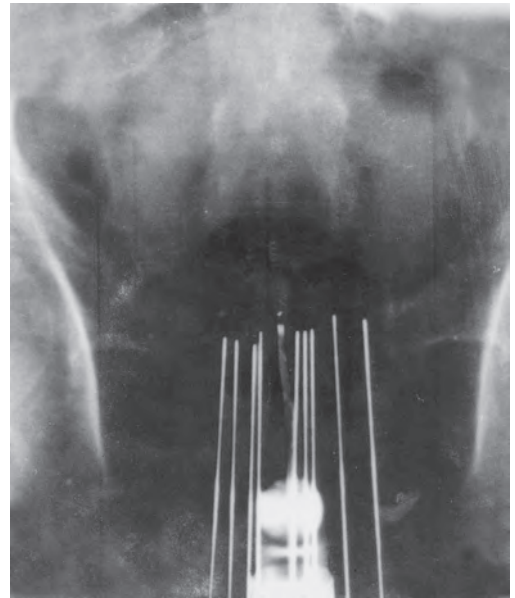


FIG. 3. X-ray shows carrier tube placement in prostate and part of microwave antenna.

TABLE 1. Treatment and evaluation schedule for 3 patient groups

	Group 1	Group 2	Group 3
No. pt	1–4, 7	5, 6, 8	9–12
Diagnosis	Prostate Ca	BPH	BPH
Therapy	TUMT, interstitial thermal mapping, radical retropubic prostatectomy 1 wk after TUMT	TUMT, interstitial thermal mapping	TUMT
Evaluation	MRI, thermal modeling, histopathology	MRI, thermal modeling	MRI, thermal modeling, posttreatment video cystoscopy, urethral histopathology

In groups 1 and 2 extensive thermal mapping was done with up to 40 transducers placed throughout prostate in addition to built-in TUMT device temperature probe.

eosin, and examined by light microscopy with prostatic mapping to determine the spread of coagulation necrosis.

In patient group 3 video cystoscopies were performed 3 weeks after microwave treatment. Samples of the prostatic urethra were taken from base to apex at the 12, 3, 6 and 9

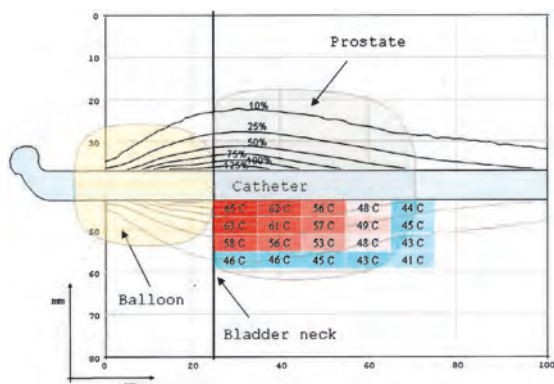


FIG. 4. Temperature distribution with schematic treatment catheter and medium sized prostate shown for clarity. Microwaves are emitted in rotational symmetrical fashion but for clarity only temperatures in lower half are shown. Necrotic area corresponds to tissue volume of approximately 20 ml. Antenna radiation pattern is shown as iso-power lines⁵ with 100% iso-curve corresponding to absorption rate of 1,000 W/kg at 50 W power output. Red and blue (10 × 4 mm) boxes indicate mean maximum temperatures at each location. Red boxes represent locations where therapeutic temperatures are achieved during typical treatment times of 15 to 30 minutes.^{7,8} Pink area 30 mm behind base represents transitional area, where necrosis may or may not develop depending on treatment time.

o'clock positions at 16 samples per patient (a total of 64 samples) and examined for the type and extent of damage. Cell kill software in the TUMT device divides the prostate

into virtual compartments and assesses the thermal exposure of each compartment from temperature readings and elapsed time. If exposure is greater than the threshold for coagulation necrosis, the compartment is considered necrotized.¹³ The same algorithm was applied to assess cell kill using temperature data from the 30 to 40 additional sensors that were inserted from the perineum. We used the Henriques⁶ and Bischof et al⁷ threshold data for cell kill analysis.

Calculated cell kill from each treatment session was compared with the volumes obtained by MRI and histopathology using statistical correlation analysis. Unit density of the prostate tissue was assumed to equalize ml and gm.

RESULTS

Thermal mapping. Thermal mapping in patient groups 1 and 2 showed that highest temperatures occurred closest to the treatment catheter, decreasing with increased radial depth and toward the apex. Therapeutic temperatures were seen up to a depth of about 12 to 15 mm from the prostatic urethra. Figure 4 was constructed to condense all temperature information obtained. It shows average peak temperatures measured throughout the prostate in patients 1 to 8. At 30 to 40 mm from the base in the apical direction temperature was generally below the threshold for causing thermal damage during typical treatment times (15 to 40 minutes). The heat field of the TUMT device can best be described as bowl-shaped with the largest circumference at the base of the prostate and the smallest circumference at the apex.

Although there were large individual variations in absolute temperatures, intraprostatic temperatures followed a general pattern (fig. 5). Initially temperature increased rapidly until a plateau was reached. The plateau effect was due to an increase in intraprostatic blood flow during the early

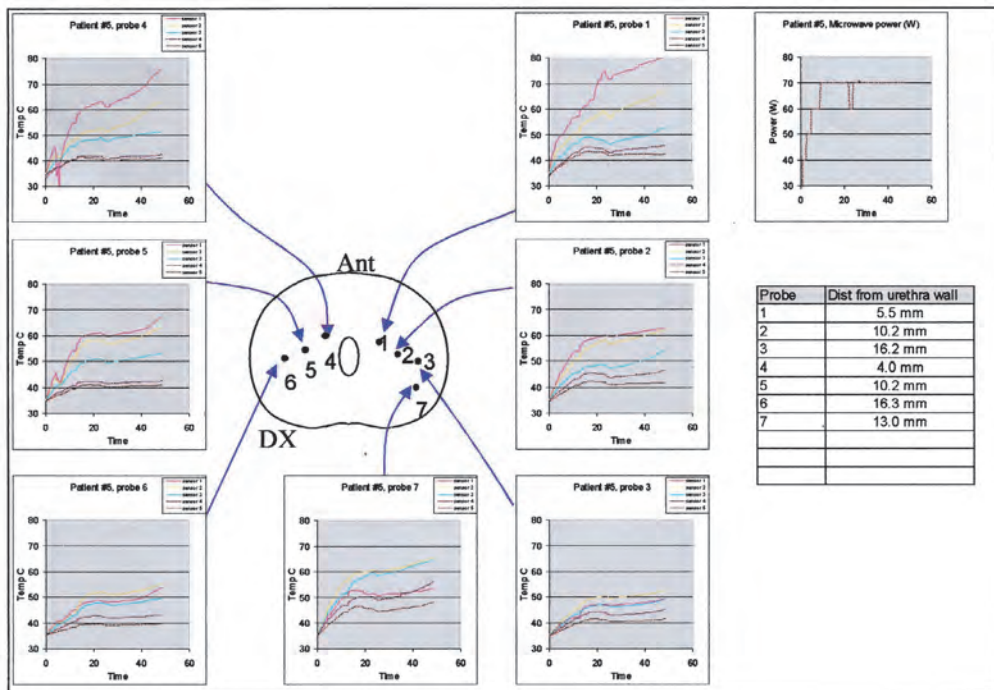


FIG. 5. Case 5. Temperature graph vs time in minutes at 35 gland locations. Temperatures were above 60C up to 10 mm from urethra. Close to urethra temperatures were above 70C. Average of 66 W microwave power were used in this patient. Pink indicates curve closest to base, followed by yellow, magenta, violet and brown in 10 mm increments. Ant, anterior. DX, dexter.

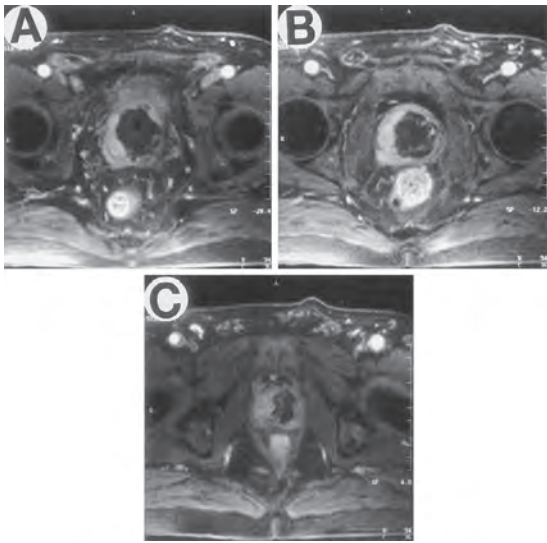


FIG. 6. Case 3. MRI of prostate base after treatment. Large dark area is perfusion defect caused by low gadolinium uptake in necrotic region. A, at base. B, 15 mm. C, 30 mm. D, toward apex.

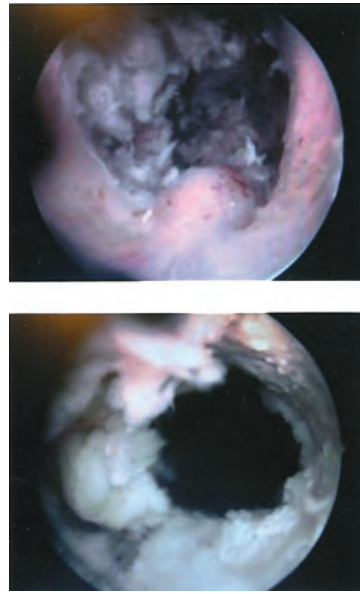


FIG. 8. Urethra 3 weeks after treatment shows necrosis extending from verumontanum to base.

phase of treatment, believed to be caused by a vasodilatation response to heat.¹⁴ Temperatures continued at the plateau until a sudden sharp increase occurred typically 15 to 30 minutes after the start. This second increase in temperature was preceded by a decrease in prostatic blood flow, believed to be caused by circulation collapse in the hottest tissue that drives the temperature because of the loss of effective tissue cooling.¹⁴ The second temperature increase marks that treatment is about to be finished since tissue necrosis now rapidly develops.

MRI. The pattern of necrosis seen on MRI showed large areas of necrosis at the base, decreasing toward the apex. Figure 6 shows a sequence of MRI slices from base to apex in 1 representative patient (3).

Histopathology. Serial whole mount sections of the 5 group 1 prostates were examined microscopically. Histology revealed sharply circumscribed heat necrosis with the non-viable zone approximately 10 to 15 mm in radius at the base

of the prostate, gradually decreasing toward the apex. Necrosis involved pure stromal nodules, mixed epithelial and stromal nodules, and epithelial nodules. Figure 7 shows pathology sections and corresponding MRI images at different locations in 2 representative patients. The pattern of coagulation necrosis seen in the histopathology findings of patient group 1 corresponded reasonably well with the pattern on MRI.

In patient group 1 more than 90% of the prostatic urethra between the base and mid gland was necrotic compared with 80% paraapically and 50% at the apex. In patient group 3, in which tissue samples were collected from the prostatic urethra, 47 of 64 samples had severe and deep necrosis (100%), 12 had moderate damage (greater than 50%) and 5 mild or superficial necrosis (less than 50%). Figure 8 shows a representative view of the urethra after treatment in group 3 with

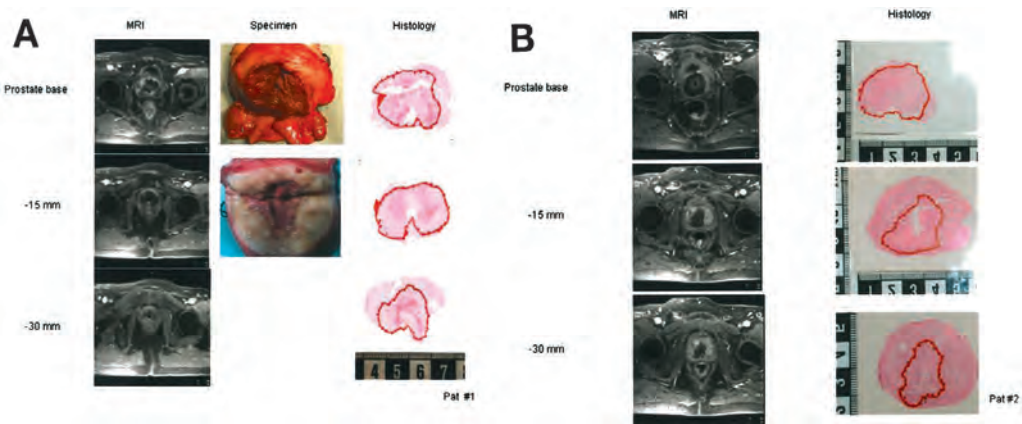


FIG. 7. MRI and corresponding histopathology at base, and 15 and 30 mm distal. Red line indicates border between viable and necrotic tissue. A, patient 1. B, patient 2.

massive necrosis along the urinary pathway from verumontanum to base.

Summary of MRI, histopathology and thermal mapping. Table 2 lists necrosis volumes found by the various techniques. In group 1 the mean volume of necrosis measured with MRI was 21 ml vs 19 for histopathology. The correlation between the 2 estimates in 5 preparations was not statistically significant ($r = 0.704$, $p = 0.185$), probably due to the limited number of cases in that group. There was a strong 1:1 correlation between MRI and the 2 means to calculate cell kill from thermal mapping according to Henriques⁶ and Bischof et al⁷ ($r = 0.837$, $p = 0.0189$ and $r = 0.864$, $p = 0.012$, respectively) in 7 preparations each with a mean value of 22 ml for MRI and 23 ml for cell kill calculations (fig. 9). There was also a statistically significant correlation between MRI and cell kill reported by the device in 12 preparations ($r = 0.582$, $p = 0.047$). The mean volume of necrosis in groups 1 to 3 measured with MRI was 20 ml, whereas the corresponding value for the device was 18 ml.

Mean necrosis volumes were similarly assessed for all 3 techniques. However, the intra-individual spread among histopathology, MRI and cell kill calculations was in the SD order of ± 10 ml.

In patient group 1 prostate cancer was generally localized in the peripheral zone at depths greater than microwave penetration, whereas the thermally damaged zone appeared in the transition zone circumferential to the prostatic urethra. The 2 zones did not generally overlap.

DISCUSSION

All 3 methods were able to detect thermally induced necrosis. The intra-individual spread in tissue volume emerged from methodological limitations. Volumetric assessment from sectional images is sensitive to how well the borders of necrosis can be defined and underestimating or overestimating a few mm may add up to considerable uncertainty. An example is TRUS, for which it has been shown that prostate volume assessment is imprecise to ± 10 ml.¹⁵ For histopathology specimen deformation and formalin shrinkage cause additional uncertainty. Cell kill calculation is based on the thermal sensitivity of tissue, which is another source of uncertainty. Still, the benefit of using cell kill calculation is obvious. It is better for the urologist to know directly during on-going treatment that, for example 30 ± 10 gm of a 100 gm prostate has been destroyed by heat than to know nothing at all.

The heat field created by the microwave antenna forms a

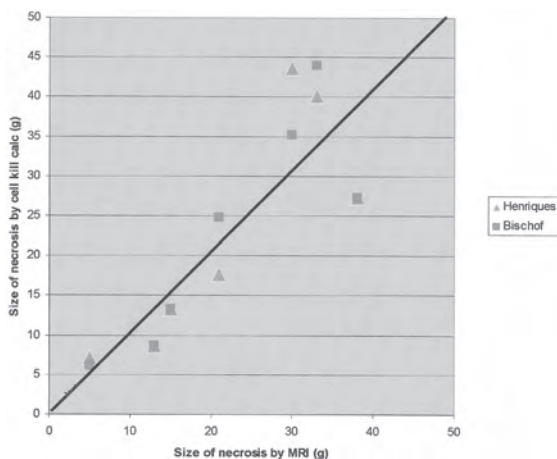


FIG. 9. Correlation between cell kill calculation and MRI^{6,7}

bow-shaped distribution through the prostate with the widest circumference at the base and the narrowest at the apex. This heating pattern is desirable since it correlates with the prostate shape and creates high temperatures for the bladder neck and 30 to 35 mm towards the apex, ie the part of the prostatic urethra where most obstruction occurs.

Intraprostatic temperature varies greatly among individuals and during the course of treatment. A decisive factor is intraprostatic blood flow, which acts as a coolant.⁵ Blood flow varies greatly among individuals¹⁶ and it changes dynamically as treatment goes on. It increases initially when heat is first applied, and decreases at the end of treatment, when coagulation necrosis occurs.^{14,17,18} Tissue temperatures mirror these changes in blood flow. Temperature saturates as blood flow peaks, and increases again rapidly as blood flow decreases toward the end of treatment. Thus, it is important to follow intraprostatic temperature during treatment and continuously adjust microwave power to compensate for changes in blood flow.^{5,19} Without this control treatment is essentially blind. From a safety aspect knowing tissue temperature is essential for decreasing the risk of over treatment.⁵

By decreasing temperature data to the more intuitive cell kill quantity treatments become interpretable. Figure 10 can

TABLE 2. Tissue necrosis volumes assessed with MRI, pathological evaluation and cell kill calculations

Pt No.	Diagnosis	TRUS Pretreatment Prostate Size (ml)	Necrosis Size (ml)		Cell Kill Necrosis Size (ml)		TUMT Device Cell Kill Vol* (ml)
			MRI	Pathological Evaluation	Henriques Threshold Curve ⁶	Bischof et al Threshold Curve ⁷	
Group 1:							
1	Ca	37	21	11	18	25	7
2	Ca	76	30	16	44	35	35
3	Ca	52	38	37	27	27	18
4	Ca	18	5	14	7	6	8
7	Ca	50	13	16	9	9	26
Group 2:							
5	BPH	62	33		40	44	20
6	BPH	42	16		5†	0†	22
8	BPH	54	15		13	13	15
Group 3:							
9	BPH	44	13				10
10	BPH	23	5				7
11	BPH	76	35				28
12	BPH	48	20				17
Means		48	20	19	23	23	18

* Based on 3 sensors.

† Because interstitial temperature probes were displaced during treatment, values are not representative.

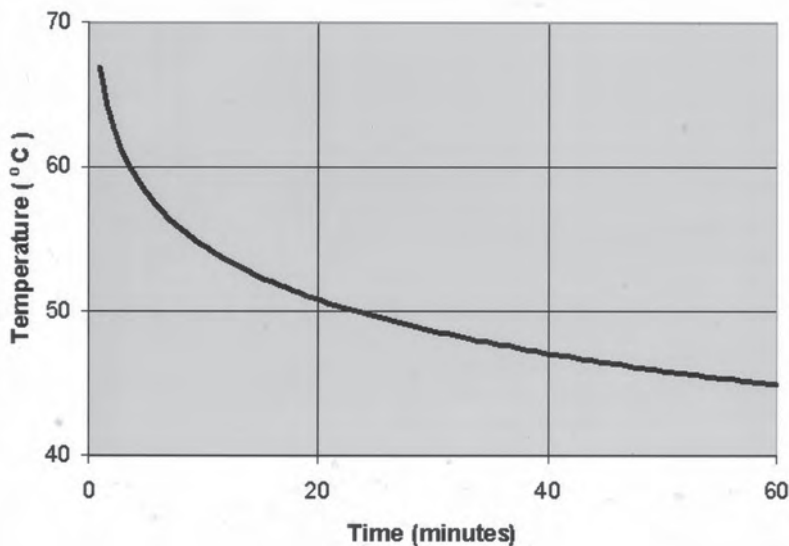


FIG. 10. Heat exposure must exceed temperature/time threshold, represented by continuous line. Area above line indicates dead cells^{6,7}

be used to see the causal connection between temperature and time. The solid line represents the threshold for creating direct cell kill by heat.^{6,7,13} To achieve successful treatment final thermal exposure should be above the solid line. By describing treatment in this way intraprostatic temperature monitoring seems to be an invaluable tool for obtaining predictable results.

Finally, this study challenges the myth that the prostatic urethra should be preserved to have effective treatment. We have not found any scientific studies that show any benefits of preserving the urethra. On the contrary, if the prostatic urethra is destroyed, it would also explain several positive observations mentioned in the literature, eg the destruction of the sensory nervous terminals in the prostatic urethra.²⁰ Pathological examinations showed that the prostatic urethra was mainly destroyed by Coretherm treatment. Studies of the clinical efficacy and safety of the device also show excellent results, comparable to those of TURP.^{2,3}

CONCLUSIONS

This study shows that microwave treatment with the TUMT device causes significant coagulation necrosis in the prostate, as evidenced by histopathology, and MRI and cell kill calculations are able to detect this necrosis with reasonable accuracy.

The cell kill program feature of the TUMT device assesses the volume of necrosis reasonably well and, thus, provides the clinician with a means to tailor treatment to each individual.

REFERENCES

- Djavan, B., de la Rosette, J., Desgrandchamps, F., Fourcade, R., Gibbon, R., Kaplan, S. et al: Interventional therapy of benign prostatic hyperplasia. In: *Proceedings of the 5th International Consultation on Benign Prostatic Hyperplasia*. Edited by C. Chaterlain, L. Denis, K. T. Foo, S. Khoury and J. McConnel. Plymouth, United Kingdom: Plymouth Distributors, Ltd., pp. 399–421, 2001
- Wagrell, L., Schelin, S., Nordling, J., Richthoff, J., Magnusson, B., Schain, M. et al: Feedback microwave thermotherapy versus TURP for clinical BPH—a randomized controlled multicenter study. *Urology*, **60**: 292, 2002
- Graber, S. F., Schmidt, D. M., Tscholl, R. and Recker, F.: ProstaLund feedback thermotherapy versus TURP in BPH: a prospectively randomized study of a novel method in comparison to the standard treatment. *J Urol, suppl.*, **167**: 363, abstract 1444, 2002
- de la Rosette, J. J. M. C. H., D'Ancona, F. C. H. and Debruyne, F. M. J.: Current status of thermotherapy of the prostate. *J Urol*, **157**: 430, 1997
- Bolmsjo, M., Stureson, C., Wagrell, L., Andersson-Engels, S. and Mattiasson, A.: Optimizing transurethral microwave thermotherapy a model for studying power, blood flow, temperature variations and tissue destruction. *Br J Urol*, **81**: 811, 1998
- Henriques, F. C.: Studies of thermal injury. *Arch Pathol*, **43**: 489, 1947
- Bischof, J. C., Bhowmick, P., Coad, J. E., Bhowmick, S., Pryor, J. L., Larson, T. et al: Heat sensitivity of human prostatic tissue: implications for thermotherapy. *J Urol, suppl.*, **169**: 287, abstract 1115, 2003
- Schelin, S.: Microwave thermotherapy in patients with benign prostatic hyperplasia and chronic urinary retention. *Eur Urol*, **39**: 400, 2001
- Hoffmann, A., Laguna, P., de la Rosette, J. J. and Wijkstra, H.: Quantification of prostate shrinkage after microwave thermotherapy: a comparison of calculated cell-kill versus 3D transrectal ultrasound planimetry. *Eur Urol*, **43**: 181, 2003
- Larson, T. R., Bostwick, D. G. and Corica, A.: Temperature-correlated histopathologic changes following microwave thermoablation of obstructive tissue in patients with benign prostatic hyperplasia. *Urology*, **47**: 463, 1996
- Larson, T. R. and Collins, J. M.: An accurate technique for detailed prostatic interstitial temperature-mapping in patients receiving microwave thermal treatment. *J Endourol*, **9**: 339, 1995
- Osman, Y. M., Larson, T. R., El-Diasty, T. and Ghoneim, M. A.: Correlation between central zone perfusion defects on gadolinium-enhanced MRI and intraprostatic temperatures during transurethral microwave thermotherapy. *J Endourol*, **14**: 761, 2000
- Bolmsjo, M., Schelin, S., Wagrell, L., Larson, T., de la Rosette, J. J. and Mattiasson, A.: Cell-kill modeling of microwave thermotherapy for treatment of benign prostatic hyperplasia. *J Endourol*, **14**: 627, 2000
- Wagrell, L., Sundin, A. and Norlén, B. J.: Intra-prostatic blood

- flow changes during feedback microwave thermotherapy measured by positron emission tomography. In: *Feedback Thermotherapy for Benign Prostatic Enlargement—A Clinical and Methodological Evaluation*. Uppsala, Sweden: Ph.D. Thesis, Uppsala University, ISBN 91-506-1383, 1999
15. Terris, M. and Stamey, T.: Determination of prostate volume by transrectal ultrasound. *J Urol*, **145**: 984, 1991
 16. Inaba, T.: Quantitative measurements of prostatic blood flow and blood volume by positron emission tomography. *J Urol*, **148**: 1457, 1992
 17. Larson, T. R. and Collins, J. M.: Increased prostatic blood flow in response to microwave thermal treatment: preliminary findings in two patients with benign prostatic hyperplasia. *Urology*, **46**: 584, 1995
 18. Floratos, D. L., Sedelaar, J. P., Kortmann, B. B., Aarnink, R. G., Wijkstra, H., Debruyne, F. M. et al: Intra-prostatic vasculature studies: can they predict the outcome of transurethral microwave thermotherapy for the management of bladder outflow obstruction? *Prostate*, **46**: 200, 2001
 19. Wagrell, L., Schelin, S., Bolmsjö, M. and Brudin, L.: Intraprostatic temperature monitoring during transurethral microwave thermotherapy for the treatment of benign prostatic hyperplasia. *J Urol*, **159**: 1583, 1998
 20. Brehmer, M., Hilliges, M. and Kinn, A. C.: Denervation of periurethral prostatic tissue by transurethral microwave thermotherapy. *Scand J Urol Nephrol*, **34**: 42, 2000